



# A microfluidic droplet system for ultra-monodisperse droplet generation: A universal approach

Ali Kalantarifard<sup>b</sup>, Elnaz Alizadeh-Haghighi<sup>a</sup>, Caglar Elbuken<sup>a,b,c,\*</sup>

<sup>a</sup> Institute of Materials Science and Nanotechnology, National Nanotechnology Research Center (UNAM), Bilkent University, Ankara 06800, Turkey

<sup>b</sup> Faculty of Biochemistry and Molecular Medicine, Faculty of Medicine, University of Oulu, 90014 Oulu, Finland

<sup>c</sup> VTT Technical Research Centre of Finland Ltd., 90570 Oulu, Finland



## HIGHLIGHTS

- Revealed the root cause for droplet volume variation in fluidic systems.
- Presented a universal novel method to achieve ultra-high monodispersity of droplets.
- The novel method implemented for the most common droplet generators and flow sources.
- Easily applicable method with no additional cost for existing droplet systems.

## ARTICLE INFO

### Article history:

Received 6 March 2022

Received in revised form 18 July 2022

Accepted 19 July 2022

Available online 22 July 2022

### Keywords:

Microfluidics  
Microdroplets  
Monodispersity  
Two phase flow  
Flow-focusing  
Coflow

## ABSTRACT

Despite the importance of droplet monodispersity, a universal methodology for high monodispersity droplet generation does not exist yet. We have recently demonstrated that unlike the conventional method of droplet generation, applying an identical pressure from a single source makes the microfluidic droplet system immune to the external fluctuations that originate from the imperfection of the flow source. In this work, we show that our method is universal and applicable to other common microfluidic devices and flow sources. We applied this method to flow-focusing and coflow devices that are commonly used for high-frequency microdroplet generation. In addition to the pressure pump, we used a syringe pump to show that our method is applicable to flow rate controllable systems as well. We compared the monodispersity of droplets formed by the conventional methods and the novel method explained in this work. © 2022 The Authors. Published by Elsevier Ltd. This is an open access article under the CC BY license (<http://creativecommons.org/licenses/by/4.0/>).

## 1. Introduction

Having control over droplet size and speed are the main advantages of droplet-based microfluidic systems over the traditional emulsification methods (Tadros, 2009). Although microfluidic systems generate monodisperse droplets with a coefficient of variation (CV) less than 3% (Zhu and Wang, 2017), achieving ultra-monodisperse droplets (CV < 1%) is still highly sought-after (Theberge et al., 2010). Today, droplet microfluidic systems have a wide variety of uses. They are replacing conventional techniques by effectively aliquoting the analyte of interest into pico to femto-liter volumes and performing the operation inside these isolated compartments. Hence, droplet monodispersity is equivalent to

the precision of this pipetting operation at a very small scale. Any uncertainty in droplet volume reflects itself in the final assay similar to using an uncalibrated micropipette. High throughput generation of monodisperse droplets is especially required for applications such as droplet digital polymerase chain reaction (Tanaka et al., 2015), biochemical analysis (Kim et al., 2012) and particle synthesis (DeMello, 2006). Droplet size and frequency depend on the microfluidic device and the flow source. For example, a flow-focusing device generates droplets at a higher rate compared to a T-junction device. Therefore, a flow-focusing device is preferable when the throughput of the system is important. On the other hand, using a T-junction device helps to achieve better control over droplet formation which makes it favorable for making monodisperse droplets. Also, depending on the application, typically either a syringe or pressure pump is used as a flow source in a microfluidic droplet system. There are different methods to improve droplet monodispersity and production rate such as using

\* Corresponding author at: Faculty of Biochemistry and Molecular Medicine, Faculty of Medicine, University of Oulu, 90014 Oulu, Finland.

E-mail address: [caglar.elbuken@oulu.fi](mailto:caglar.elbuken@oulu.fi) (C. Elbuken).

a pulseless syringe pump (Crawford et al., 2017), integration of compliance (Kalantarifard et al., 2018; Kang and Yang, 2012; Pang et al., 2014) or a feedback system (Crawford et al., 2017), design of 3-D flow-focusing geometry (Jeong et al., 2012), and parallelization of droplet generators in multilayer chip that have been used. Yet, these approaches suffer from fabrication and experimental complexity, long response time, limited portability and do not lead to a practical and cost-effective method to obtain ultra-monodisperse droplets at a high production rate.

In our previous study (Kalantarifard et al., 2021), we showed that ultra-monodisperse droplet generation with a coefficient of variation close to the theoretical limit of 0% CV is achievable by (i) supplying the inlets pressure from the same source, (ii) lowering the interfacial tension, (iii) decreasing hydrodynamic resistance of the main channel that accommodates the droplets and (iv) equating inlet channels hydrodynamic resistance. We applied these rules to a T-junction microfluidic device and used a pressure pump as a flow source. We generated microdroplets with a monodispersity of less than 0.2% CV and a droplet generation rate near 10 Hz (Kalantarifard et al., 2021).

Here, we study droplet monodispersity using flow-focusing and coflow devices that have a higher droplet generation frequency compared to a T-junction device. We supply continuous and dispersed phases from a single source using pressure or syringe pump. We compare the CV of droplet sizes formed by the conventional method and the method following our design guidelines. The results confirm the significant improvement in droplet monodispersity by applying our design guidelines. Additionally, the results verify that regardless of the flow source performance, applying an identical pressure/flow rate from a single source makes the microfluidic droplet system immune to the external fluctuations that originate from the imperfection of the flow source. Note that using a flow-focusing and coflow device instead of a T-junction results in both high monodispersity and high throughput droplet systems. These results show the universality of our method for making ultra-monodisperse droplets that can be used for different geometries (T-junction, flow-focusing and coflow) and common flow sources such as pressure and syringe pump.

## 2. Results and discussions

### 2.1. Monodisperse droplet generation using a flow-focusing device and pressure pump

In our previous study (Kalantarifard et al., 2021), we demonstrated that for a T-junction device, (i) applying identical pressure to the fluids, (ii) increasing inlet pressure, (iii) lowering the hydrodynamic resistance of the main channel ( $R_m$ ) and (iv) having equal hydrodynamic resistances for both inlet channels ( $R_c = R_d$ ) results in ultra-monodisperse droplet generation. The underlying principle is that when the inlet pressures are equated, the flow rate ratio of dispersed and continuous phases is independent of the inlet pressure, as shown in Fig. 1. Herein, we apply these guidelines for a flow-focusing device. A flow-focusing droplet generator PDMS/glass chip (all channels with 150  $\mu\text{m}$  width and 100  $\mu\text{m}$  height) is designed for ultra-monodisperse droplet generation. Using a pressure pump, DI water and silicone oil (10 mPa.s) are introduced to the microfluidic device as dispersed and continuous phase, respectively. The interfacial tension between the two fluids is  $\gamma = 38 \text{ mN/m}$ .

As given in Fig. 1, in the conventional method, two different ports of the pressure generator are utilized to drive the continuous and dispersed phases. For the single source configuration, a bifurcating tubing connector is used to apply the same pressure for the two phases ( $P_c, P_d$ ). Then, to adjust the droplet size, the hydrodynamic resistance ratio can be controlled either by design or using real-time valving options (Kalantarifard et al., 2021). It is to note that hydrodynamic resistance of the inlet channels are composed of a tubing resistance ( $R_{ct}$ ) and a channel resistance ( $R_{cm}$ ). In our case, due to relatively larger inner diameter of the tubing with respect to channel cross section, the tubing resistances were negligible ( $R_{ct} \ll R_{cm}$ ). Using conventional and single source configuration, we investigated the effect of applying identical pressure and pressure enhancement on droplet monodispersity. For both systems, the continuous phase was introduced at four different pressures ( $P_c = 400, 450, 500, 550 \text{ mbar}$ ). To achieve a stable pattern of droplet generation, the recording was started 3 min after applying

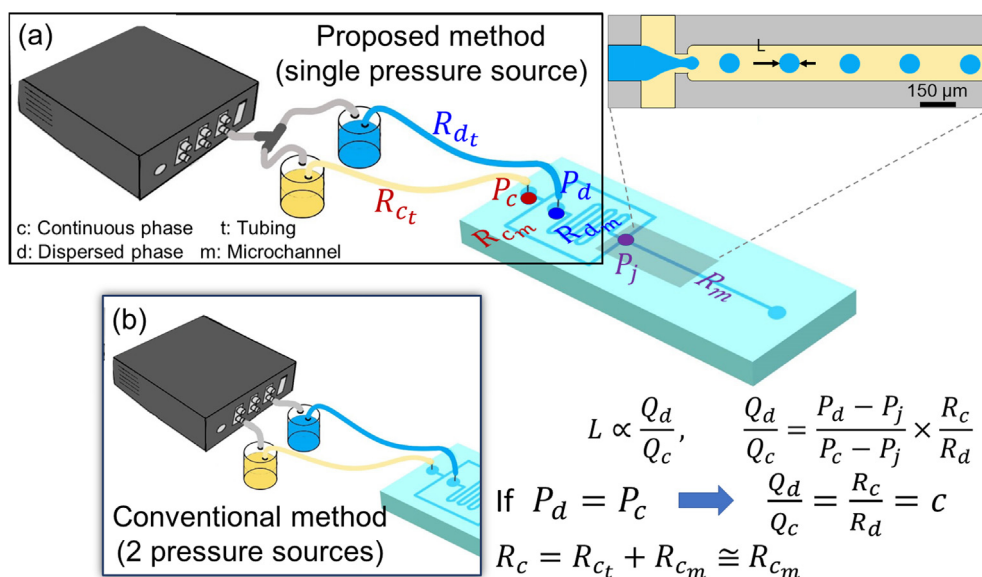


Fig. 1. Schematic representation of the (a) proposed and (b) conventional method for supplying fluids to a flow-focusing device using a pressure pump.

the set pressure. The droplet generation videos were recorded by a high-speed camera. Afterwards, Droplet Morphometry and Velocimetry (DMV) software (Basu, 2013) was used to obtain the coefficient of variation (CV%) for at least 400 droplets. For four inlet pressure values, the CV% results of the recommended single source configuration ( $P_d = P_c$ ) and conventional method ( $P_d = P_c$  and  $P_d \neq P_c$ ) are obtained as summarized in Fig. 2.

As illustrated in Fig. 2, if the conventional method is used (two pressure sources) the CV% for the identical pressure ( $P_d = P_c$ ) is lower than different continuous and dispersed phase pressures ( $P_d \neq P_c$ ). This is due to the lower effect of external fluctuations on inlet flow rate ratios for identical inlet pressure case. Note that this effect is more significant at the lowest pressure in which the external fluctuation is higher (Glawdel and Ren, 2012). Running the system away from  $P_{d,min}$  reduces fluctuations (Glawdel and Ren, 2012). The application of single-source configuration results in smaller CV% values than the conventional method in every applied pressure. For the identical inlet pressures case, the higher CV% value of using two pressure sources rather than a single source is due to the asynchronous perturbations that inevitably originate from the flow source. Indeed, using a single pressure source leads to simultaneous external fluctuations of continuous and dispersed phase fluids at the junction of the microfluidic device. The distribu-

tion of the normalized size of 400 droplets shows the effect of using a single pressure source on monodispersity (Fig. 2b). Furthermore, as demonstrated in Fig. 2, the CV% values decrease with increasing inlet pressure. Increasing inlet pressure/flow rate results in a higher capillary number. As shown in the previous studies, pressure fluctuation decreases by increasing capillary number (Kalantarifard et al., 2021; Romero and Abate, 2012). Thus, as can also be deduced from Fig. 2, higher monodispersity is achieved by applying higher inlet pressures.

=Another way to improve the droplet monodispersity is to optimize the channel network design. Next, the effect of decreasing the main channel length (equivalent to a decrease in  $R_m$ ) on droplet monodispersity has been studied. This is equivalent to increasing inlet pressure, since junction pressure increases for shorter main channel lengths. As demonstrated in Fig. 3, thanks to the micro plug valve integration (Guler et al., 2017), a flow-focusing device with five discrete main channel lengths has been utilized to generate droplets. The serpentine section of the main channel was punched at four different locations and equipped with micro plug valves. All valves are placed in an open position initially. To obtain the desired channel length, one of the valves has been removed and the corresponding hole has been used as the outlet. This method provides 5 different main channel lengths ( $L_m = 5, 7.5, 10, 12.5$  and  $15$  cm) on the same microfluidic chip and allows a precise measurement in comparison to a setting when multiple devices with different main channel lengths were used.

The droplet monodispersity improves with decreasing main channel length, as shown in Fig. 3. For the shortest main channel ( $L_m = 5$  cm), a CV of 0.43% was obtained. Furthermore, the number of droplets inside the main channel decreases as the main channel shortens, which leads to further reduction of  $R_m$ . As a result, the monodispersity improves by keeping the main channel length short enough to minimize the number of droplets and consequently the effect of internal pressure fluctuations. More importantly, the hydrodynamic resistance of a longer main channel is more susceptible to change due to the presence of debris, fabrication imperfections and surface treatment of the channel. Therefore, not only a longer main channel leads to higher CV, but also it is more prone to experimental uncertainties.

Another way to improve droplet monodispersity by channel network design is to equate the hydrodynamic resistance of the dispersed and continuous phase inlet channels ( $R_c = R_d$ ). For this purpose, the same flow-focusing design with a main channel length of 15 cm was used, as demonstrated in Fig. 4. The  $R_c/R_d$  ratio was varied by moving up or down a screw valve mounted on the serpentine section of the dispersed phase channel (Elizabeth Hulme et al., 2009).

Tightening the screw resulted in decreasing channel height and consequently increasing hydrodynamic resistance ( $R_d$ ) of the dispersed phase channel. Using image processing, quantitative values of  $R_c/R_d$  were obtained by measuring the volume ratio of the dispersed phase to the continuous phase in the main channel. The screw rotation angles of  $\theta^\circ = 0, 30, 60, 90, 120, 135$  and  $150$  were set to vary  $R_c/R_d$  by changing the height of the dispersed phase channel. Tightening the screw with a rotation angle of  $\theta^\circ = 120$ , which approached to  $R_c/R_d = 0.28$ , resulted in the smallest experimental CV%, as shown in Fig. 4. The experimental results given in Figs. 2–4 indicate that using the proposed design guidelines results in ultra-monodisperse droplets.

## 2.2. Monodisperse droplet generation using a flow-focusing device and a syringe pump

A syringe pump is a common flow source used in microfluidic droplet systems to supply fluids at a desired flow rate. As showed

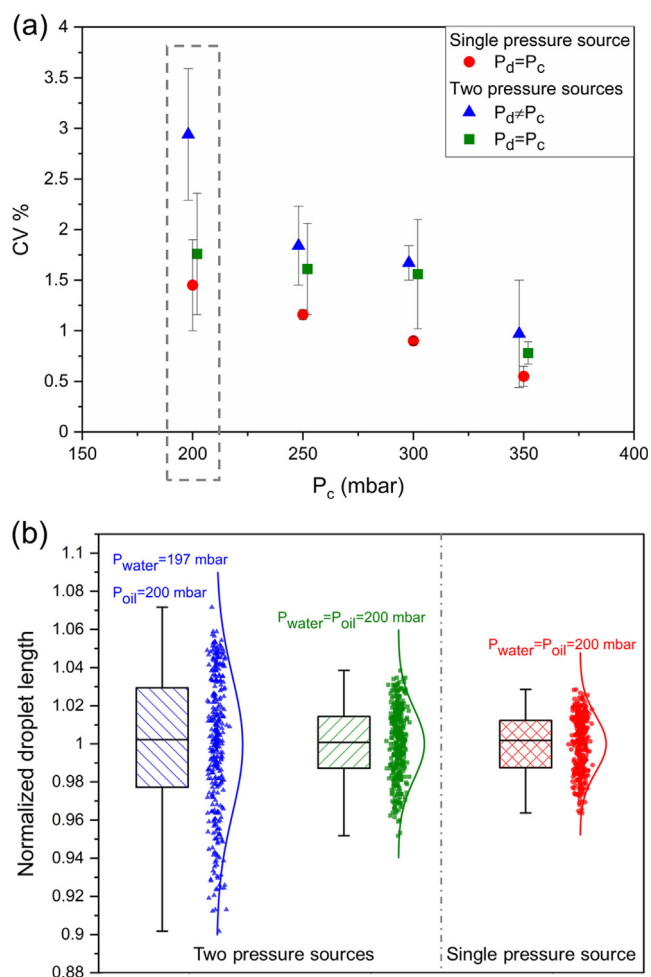


**Fig. 2.** (a) Experimental results of droplet monodispersity in different applied pressures. (b) Distribution of normalized size of individual droplets for a single and two pressure sources configuration when  $P_c = 200$  mbar, denoted with a dashed box in (a). For the unequal pressure case ( $P_d \neq P_c$ ), which is demonstrated as blue triangle, the pressure of the dispersed and continuous phase is set as  $P_d = 0.985 P_c$ . (For interpretation of the references to colour in this figure legend, the reader is referred to the web version of this article.)

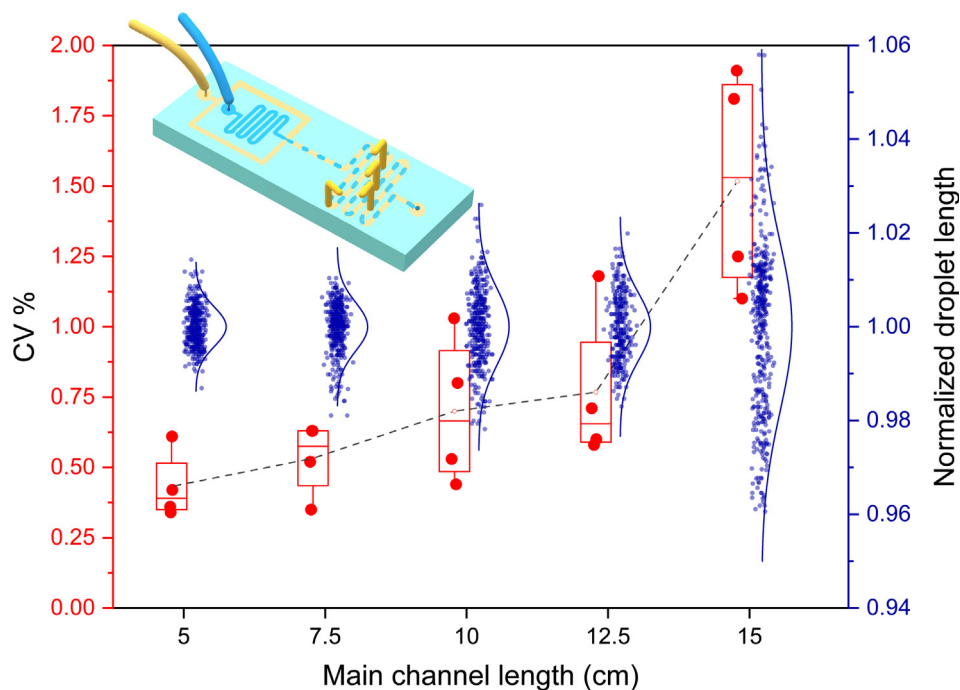


**Fig. 3.** Droplet monodispersity, CV% (left) and normalized droplet length (right) results as a function of main channel length ( $L_m$ ). The experiments were performed at four iterations. Droplets obtained in a single run are demonstrated as blue dots. The chip is equipped with micro plug valves that allow modification of main channel in five different lengths. The red circles and boxes show CV% value at each iteration and distribution of CV% values, respectively. The dashed line which connects the mean value of CV% at each  $L_m$  shows the effect of main channel length on the droplet monodispersity. (For interpretation of the references to colour in this figure legend, the reader is referred to the web version of this article.)

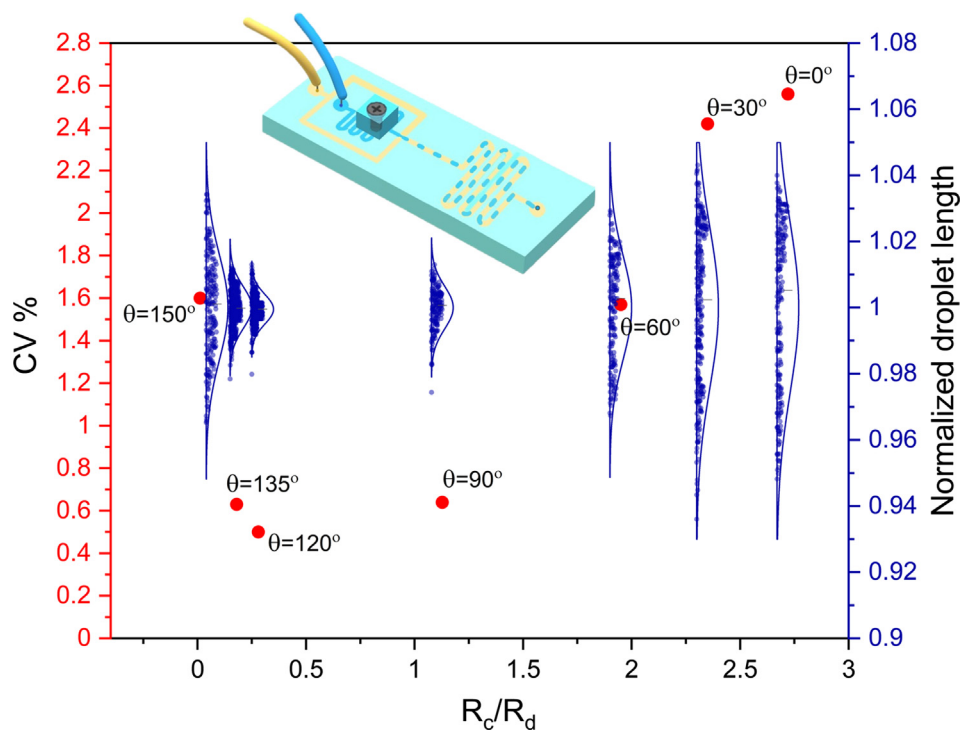


**Fig. 4.** Experimental results of droplet monodispersity, CV% (left) and normalized droplet length (right) as a function of hydrodynamic resistance ratio ( $R_c/R_d$ ) of inlet channels for the flow-focusing device equipped with the screw valve. Every  $R_c/R_d$  corresponds to a certain rotation angle ( $\theta$ ) of the screw. The normalized size of 400 individual droplets is shown where a blue dot represents an individual droplet. (For interpretation of the references to colour in this figure legend, the reader is referred to the web version of this article.)

in the previous section, for the pressure pump driven system, ultra-monodispersity was achieved when  $R_c/R_d = 1$  and a single source was used to drive both dispersed and continuous phase at equal

pressure. Indeed, based on the Hagen-Poiseuille law, these conditions are equivalent to having an equal flow rate for the dispersed and continuous phase ( $Q_d = Q_c$ ). Here, the effect of using a single

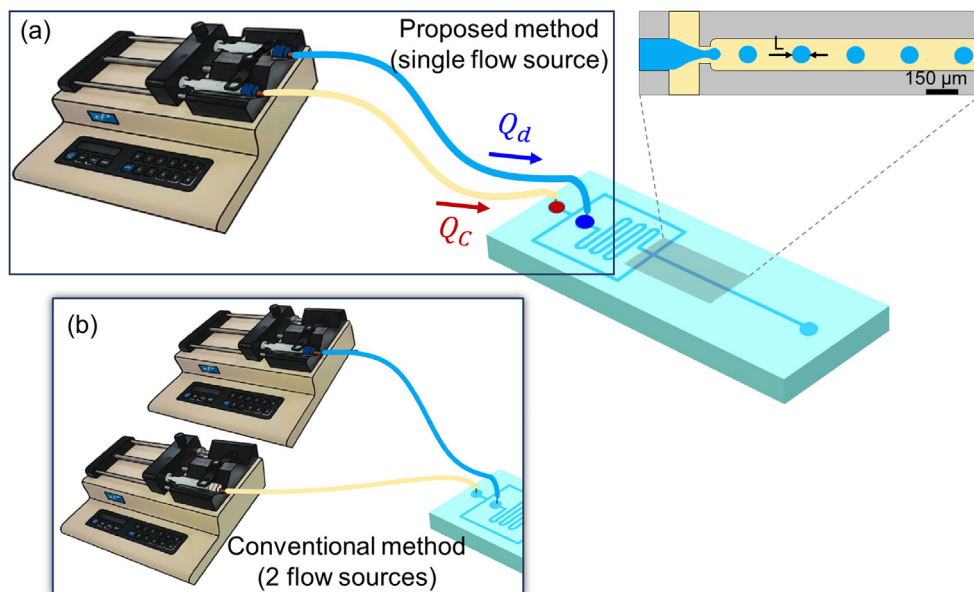


**Fig. 5.** Schematic representation of the proposed (a) and conventional (b) method for supplying fluids to a flow-focusing device using a syringe pump as a flow source.

syringe pump to drive both continuous and dispersed phases equally is studied and compared with the conventional method when two syringe pumps are used to supply the fluids. Both single source and conventional methods of supplying fluid are demonstrated in Fig. 5.

For the single source configuration, the two syringes with the same volume of 5 ml were placed in the same syringe pump and identical flow rates of  $Q_d = Q_c = 1, 1.5, 2, 2.5 \mu\text{l}/\text{min}$  were applied. In the conventional method, two different syringe pumps are used to drive the fluids for equal ( $Q_d = Q_c$ ) and different ( $Q_d \neq Q_c$ ) flow rate. The effect of increasing flow rate on droplet monodispersity and the difference between the application of a single source and two sources are studied. The system ran for 10 min after adjusting the input flow rates to obtain a stable droplet formation. To reach stability a longer time is used in comparison to pressure pump experiments due to the slower response time of displacement pumps (Glawdel and Ren, 2012; Saateh et al., 2019). The CV% results for three cases (single source  $Q_d = Q_c$ , two sources  $Q_d = Q_c$  and  $Q_d \neq Q_c$ ) are demonstrated for four different inlet flow rates in Fig. 6.

center000Similar to the pressure pump case using a single syringe pump results in droplet monodispersity improvement (Fig. 6) and if the conventional method is used (two flow rate sources) the CV% for the identical flow rate ( $Q_d = Q_c$ ) is lower than that with a different flow rate of the continuous and dispersed phase ( $Q_d \neq Q_c$ ). A syringe pump induces high external fluctuation in the microfluidic droplet system compared to a pressure pump (Li et al., 2014; Zeng et al., 2015). Note that as in the pressure pump case, the external fluctuation is more significant at droplet formation using lower flow rates. Therefore, the effect of using a single flow source for a syringe pump case is much higher than a pressure pump case at especially a low flow rate. Increasing flow rate resulted in smaller CV% values which is in line with our results with the pressure pump. However, the rationale behind these results is different. In the syringe pump case, the flow rate is inversely correlated with the mechanical oscillations of the step motor in the syringe pump. Therefore, the amplitude of oscillation decreases with increasing flow rate (Korczyk et al., 2011; Zeng et al., 2015).

To dampen the external hydrodynamic fluctuations, we applied elastomeric off-chip tubing which leads to steady flow rates (Kalantarifard et al., 2018). Here, the flexible silicone tubing

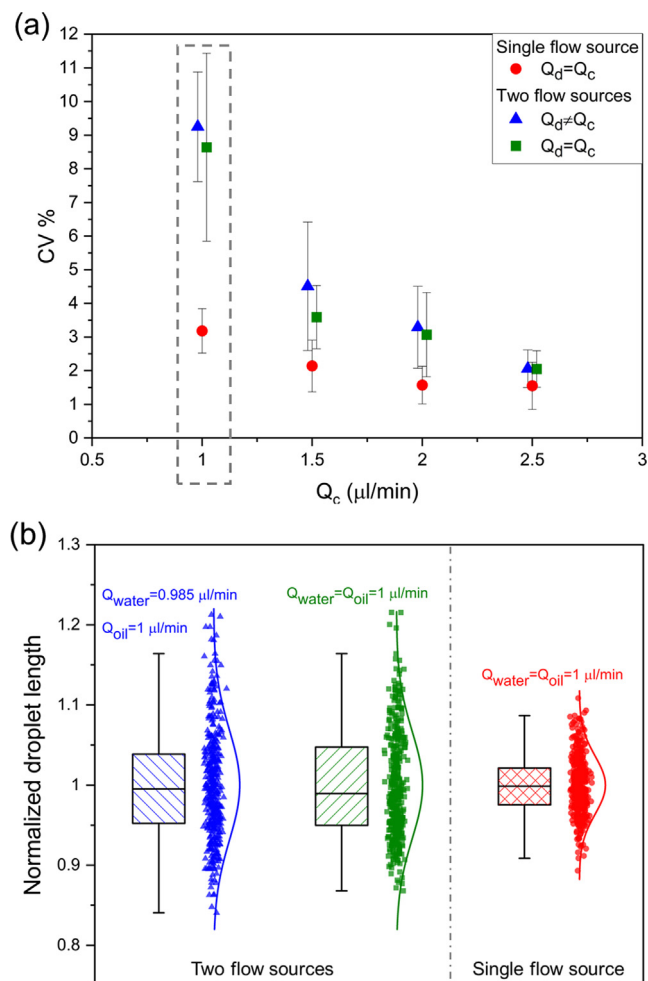


**Fig. 6.** (a) Experimental results of droplet monodispersity values in different applied flow rates. (b) Distribution of normalized size of individual droplets for single and two flow sources configuration when  $Q_c = 1 \mu\text{l}/\text{min}$ , denoted with a dashed box in (a). For the unequal flow rate case ( $Q_d \neq Q_c$ ), which is demonstrated as blue triangle, the flow rate of the dispersed and continuous phase is set as  $Q_d = 0.985 Q_c$ . (For interpretation of the references to colour in this figure legend, the reader is referred to the web version of this article.)

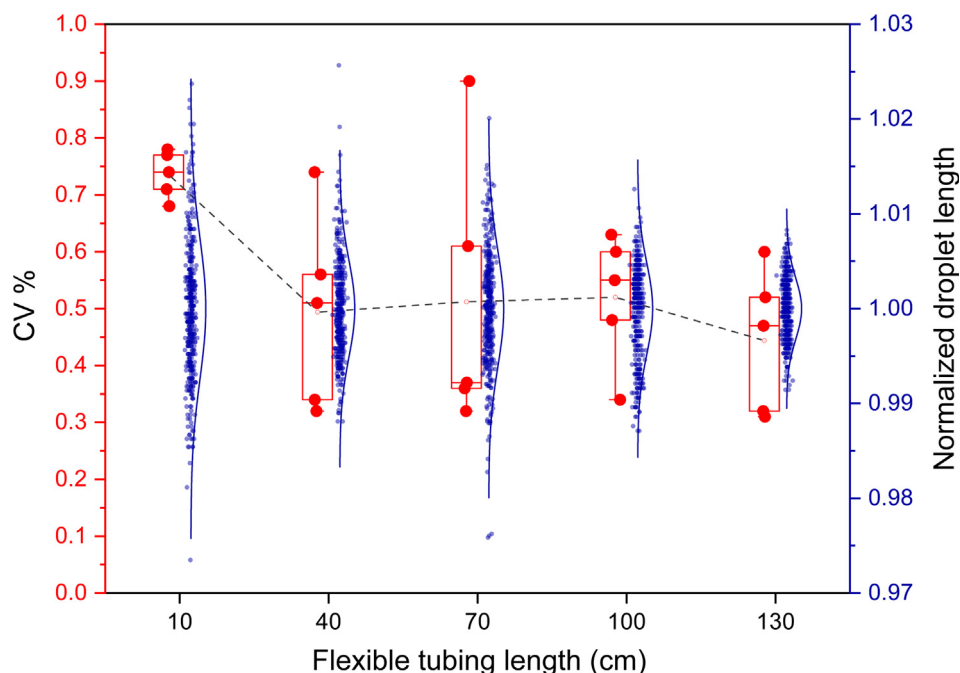


**Fig. 7.** Droplet monodispersity, CV% (left) and normalized droplet length (right) results as a function of flexible tubing lengths for the applied 1  $\mu\text{l}/\text{min}$  flow rate. The experiments were performed at five iterations. Droplets obtained in a single run are demonstrated as blue dots. The red circles and boxes show CV% value at each iteration and distribution of CV% values, respectively. The dashed line which connects the mean value of CV% at each tubing length shows the effect of tubing length on the droplet monodispersity. (For interpretation of the references to colour in this figure legend, the reader is referred to the web version of this article.)

(Cole-Parmer) with 0.8 mm inner diameter and 2.4 mm outer diameter in five different lengths (10, 40, 70, 100, 130 cm) was used on the single flow source to obtain higher droplet monodispersity. The effect of flexible tubings on droplet monodispersity for 1  $\mu\text{l}/\text{min}$  flow rate is demonstrated in terms of CV% and normalized droplet length in Fig. 7.

As shown in Fig. 7, the droplet monodispersity is improved by increasing the length of the flexible tubing. However, the improvement is marginal since the CV% results for the case with a single flow source is already very low. Note that although the shorter flexible tubing leads to higher CV%, it is less prone to experimental disturbance (as shown in red boxes in Fig. 7), possibly due to vibrations in the experimental setup.

### 2.3. Monodisperse droplet generation using a coflow device

To confirm the universality of our method we generated microdroplets with a coflow device which has a different structure than T and cross junction devices using conventional and the method following our design guidelines. The coflow microfluidic device was fabricated by coaxially inserting a cylindrical glass capillary with 200  $\mu\text{m}$  inner diameter (dispersed phase capillary) into a tapered one (continuous phase capillary) with 600  $\mu\text{m}$  inner diameter. Then, the dispersed phase and continuous capillaries were inserted into a PDMS cylindrical channel with 1.4 mm inner diameter. The hydrodynamic resistance of the main channel that accommodates the droplets in the coflow device is extremely low. Therefore, the third design guideline of the method (low main channel resistance), which has a significant effect on the internal fluctuation, is already satisfied and compared to a flow-focusing device CV% results is much lower for coflow device (Fig. 8). Again, a pressure and a syringe pump were used as flow sources to supply fluids. Although due to the structure of the coflow device, droplet formation with equal flow rate was not possible, using two syr-

inges in different diameters we could supply flow rate from a single syringe pump and compare our method with the conventional method (Fig. 8(b)). Applying pressure/flow rate from a single source and using a structure with an extremely low hydrodynamic resistance of the main channel minimized the effect of external and internal fluctuation on droplet monodispersity, respectively. As shown in Fig. 8, for the case with minimum effect of external and internal fluctuation, the CV% results do not change with increasing pressure/flow rate. However, still applying pressure/flow rate from a single source improves droplet monodispersity.

### 2.4. Droplet monodispersity for various two-phase combinations

The proposed method is independent of physical properties such as viscosity, density, and interfacial tension between the two immiscible fluids. Finally, this was confirmed by using several combinations of fluids with different physical properties to demonstrate the universality of the proposed method. The method was also tested for both water in oil (W/O) and oil in water (O/W) droplets. These experiments were performed using pressure pumps and the conventional (two sources) and proposed method (single source) of supplying fluids. The results are provided in Table 1, where  $c$  and  $d$  denote continuous and dispersed phases respectively.  $P$ ,  $\rho$ ,  $\mu$ , and  $\sigma$  are applied pressure, density, viscosity, and interfacial tension between fluids. The interfacial tensions between fluids were measured using Kruss DSA25B tensiometer. As given in Table 1, six different combinations of fluids were used for droplet generation. Droplet monodispersity in all cases using the proposed supplying method is better than that using the conventional method. Note that the given CV% values of the conventional method in the Table 1, are for identical pressure and it would be a higher value if we apply unequal pressure. Normally, in the conventional supplying method the fluids are supplied to the chip at different pressures.

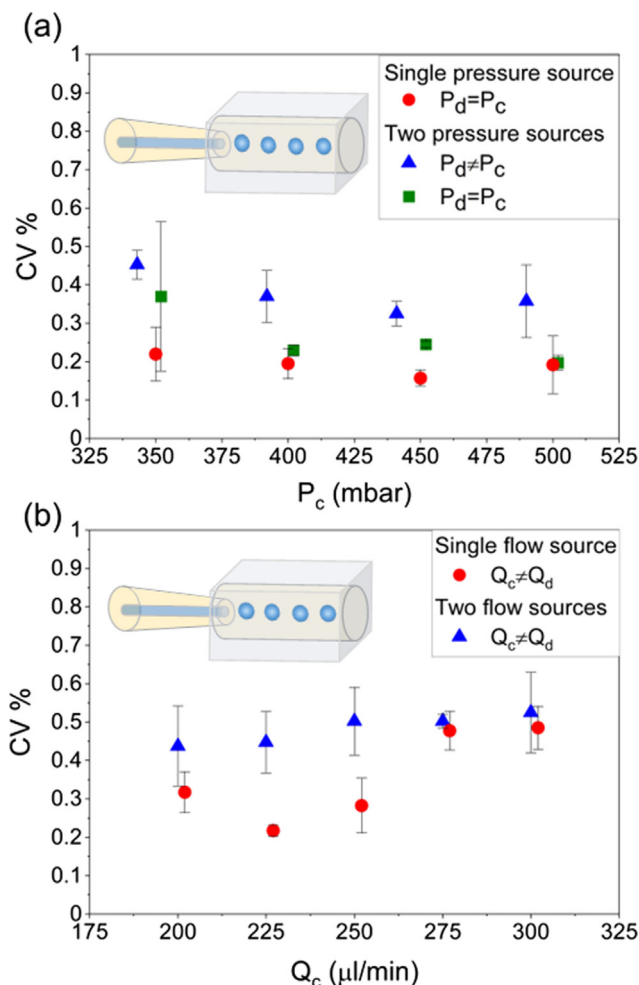


**Fig. 8.** (a) Experimental results of pressure pump generated droplet monodispersity in different applied pressures for single and two flow sources configuration. For the unequal pressure case, which is demonstrated as blue triangle, the pressure of the dispersed and continuous phase is set as  $P_d = 0.98P_c$ . (b) Experimental results of syringe pump generated droplet monodispersity values in different applied flow rates for single and two flow sources configuration when  $Q_c = 10.5Q_d$ . (For interpretation of the references to colour in this figure legend, the reader is referred to the web version of this article.)

**Table 1**

Droplet monodispersity comparison for the conventional and proposed method using pressure driven flow for different combinations of fluids and droplet types. CV% values were obtained for 400 droplets.

Method	Dispersed phase	Continuous phase	$P$ (mbar)	$\rho_d$ (gr/cm <sup>3</sup> )	$\rho_c$ (gr/cm <sup>3</sup> )	$\mu_d$ (mpa.s)	$\mu_c$ (mpa.s)	$\sigma$ (mN/m)	Droplet size ( $\mu\text{m}$ )	Droplet type	CV%
Two sources	DI water	SF 10	200	0.996	0.93	0.9	10	25	132	W/O	1.166
Single source									130		0.603
Two sources		Mineral oil	200	0.996	0.86		30	28	306		0.636
Single source									340		0.297
Two sources		SF 100	300	0.996	0.96		100	25	227		1.35
Single source									295		0.82
Two sources		Hexadecane	100	0.996	0.77		3.6	43	121		0.67
Single source									123		0.49
Two sources	DI water+Glycerol	SF 10	200	1.15	0.93	9	10	20.14	125		1.57
Single source									130		1.12
Two sources	SF 10	DI water+3% PVA	70	0.93	1.073	10	7.25	23.2	136.9	O/W	2.08
Single source									132.9		1.12

### 3. Conclusion

In this study, we showed that using a single supply source is an optimal solution to obtain high droplet monodispersity regardless of a droplet generator design and a flow source used for droplet generation. Doing so, we achieved a droplet monodispersity of 0.5% CV using a flow-focusing device. Furthermore, the droplet generation frequency was improved from 10 Hz to 100 Hz using a flow-focusing device instead of a T-junction. Also, the method was tested for both O/W and W/O droplets various continuous and dispersed phase fluid combinations and yielded monodispersity improvement in all scenarios. These results together with our results on the T-junction droplet generator verify the single source technique as a universal method that can be applied to common microfluidic devices. Additionally, we compared the performance of common flow sources (pressure and syringe pump) in terms of droplet monodispersity while using the offered guidelines. We confirmed that our proposed method is valid for both common drive units, regardless of their quality.

#### CRediT authorship contribution statement

**Ali Kalantarifard:** Methodology, Investigation, Validation, Visualization, Writing – original draft. **Elnaz Alizadeh-Haghighi:** Visualization. **Caglar Elbuken:** Methodology, Validation, Project administration, Funding acquisition, Supervision, Writing – review & editing.

#### Data availability

Data will be made available on request.

#### Declaration of Competing Interest

The authors declare that they have no known competing financial interests or personal relationships that could have appeared to influence the work reported in this paper.

#### Acknowledgements

This work was supported by Academy of Finland grant no. 342448. This research is connected to the DigiHealth-project, a

strategic profiling project at the University of Oulu and partially supported by the Academy of Finland (project no. 326291) and the University of Oulu. The authors thank Mostafa Bakouei for discussions and his help in experiments.

## References

- Basu, A.S., 2013. Droplet morphometry and velocimetry (DMV): A video processing software for time-resolved, label-free tracking of droplet parameters. *Lab Chip* 13, 1892–1901. <https://doi.org/10.1039/c3lc50074h>.
- Crawford, D.F., Smith, C.A., Whyte, G., 2017. Image-based closed-loop feedback for highly mono-dispersed microdroplet production. *Sci. Rep.* 7, 1–9. <https://doi.org/10.1038/s41598-017-11254-5>.
- DeMello, A.J., 2006. Control and detection of chemical reactions in microfluidic systems. *Nature* 442, 394–402. <https://doi.org/10.1038/nature05062>.
- Elizabeth Hulme, S., Shevkoplyas, S.S., Whitesides, G.M., 2009. Incorporation of prefabricated screw, pneumatic, and solenoid valves into microfluidic devices. *Lab Chip* 9, 79–86. <https://doi.org/10.1039/b809673b>.
- Glawdel, T., Ren, C.L., 2012. Global network design for robust operation of microfluidic droplet generators with pressure-driven flow. *Microfluid. Nanofluidics* 13, 469–480. <https://doi.org/10.1007/s10404-012-0982-y>.
- Guler, M.T., Beyazkiliç, P., Elbuken, C., 2017. A versatile plug microvalve for microfluidic applications. *Sensors Actuators, A Phys.* 265, 224–230. <https://doi.org/10.1016/j.sna.2017.09.001>.
- Jeong, W.C., Lim, J.M., Choi, J.H., Kim, J.H., Lee, Y.J., Kim, S.H., Lee, G., Kim, J.D., Yi, G.R., Yang, S.M., 2012. Controlled generation of submicron emulsion droplets via highly stable tip-streaming mode in microfluidic devices. *Lab Chip* 12, 1446–1453. <https://doi.org/10.1039/c2lc00018k>.
- Kalantarifard, A., Alizadeh-Haghighi, E., Saateh, A., Elbuken, C., 2021. Theoretical and experimental limits of monodisperse droplet generation. *Chem. Eng. Sci.* 229, <https://doi.org/10.1016/j.ces.2020.116093> 116093.
- Kalantarifard, A., Alizadeh Haghighi, E., Elbuken, C., 2018. Damping hydrodynamic fluctuations in microfluidic systems. *Chem. Eng. Sci.* 178, 238–247. <https://doi.org/10.1016/j.ces.2017.12.045>.
- Kang, Y.J., Yang, S., 2012. Fluidic low pass filter for hydrodynamic flow stabilization in microfluidic environments. *Lab Chip* 12, 1881–1889. <https://doi.org/10.1039/c2lc21163g>.
- Kim, J.Y., Cho, S.W., Kang, D.K., Edel, J.B., Chang, S.I., Demello, A.J., O'Hare, D., 2012. Lab-chip HPLC with integrated droplet-based microfluidics for separation and high frequency compartmentalisation. *Chem. Commun.* 48, 9144–9146. <https://doi.org/10.1039/c2cc33774f>.
- Korczyk, P.M., Cybulski, O., Makulska, S., Garstecki, P., 2011. Effects of unsteadiness of the rates of flow on the dynamics of formation of droplets in microfluidic systems. *Lab Chip* 11, 173–175. <https://doi.org/10.1039/c0lc00088d>.
- Li, Z., Mak, S.Y., Sauret, A., Shum, H.C., 2014. Syringe-pump-induced fluctuation in all-aqueous microfluidic system implications for flow rate accuracy. *Lab Chip* 14, 744–749. <https://doi.org/10.1039/c3lc51176f>.
- Pang, Y., Kim, H., Liu, Z., Stone, H.A., 2014. A soft microchannel decreases polydispersity of droplet generation. *Lab Chip* 14, 4029–4034. <https://doi.org/10.1039/c4lc00871e>.
- Romero, P.A., Abate, A.R., 2012. Flow focusing geometry generates droplets through a plug and squeeze mechanism. *Lab Chip* 12, 5130–5132. <https://doi.org/10.1039/c2lc40938k>.
- Saateh, A., Kalantarifard, A., Celik, O.T., Asghari, M., Serhatlioglu, M., Elbuken, C., 2019. Real-time impedimetric droplet measurement (iDM). *Lab Chip* 19 (22), 3815–3824.
- Tadros, T.F., 2009. Emulsion science and technology. *Emuls. Sci. Technol.* <https://doi.org/10.1002/9783527626564>.
- Tanaka, H., Yamamoto, S., Nakamura, A., Nakashoji, Y., Okura, N., Nakamoto, N., Tsukagoshi, K., Hashimoto, M., 2015. Hands-off preparation of monodisperse emulsion droplets using a poly(dimethylsiloxane) microfluidic chip for droplet digital PCR. *Anal. Chem.* 87, 4134–4143. <https://doi.org/10.1021/ac503169h>.
- Theberge, A.B., Courtois, F., Schaerli, Y., Fischlechner, M., Abell, C., Hollfelder, F., Huck, W.T.S., 2010. Microdroplets in microfluidics: An evolving platform for discoveries in chemistry and biology. *Angew. Chemie - Int. Ed.* 49, 5846–5868. <https://doi.org/10.1002/anie.200906653>.
- Zeng, W., Jacobi, I., Beck, D.J., Li, S., Stone, H.A., 2015. Characterization of syringe-pump-driven induced pressure fluctuations in elastic microchannels. *Lab Chip* 15, 1110–1115. <https://doi.org/10.1039/c4lc01347f>.
- Zhu, P., Wang, L., 2017. Passive and active droplet generation with microfluidics: a review. *Lab Chip* 17, 34–75. <https://doi.org/10.1039/C6LC01018K>.